

SCIENTIFIC REPORTS



OPEN

Photo-flocculation of microbial mat extracellular polymeric substances and their transformation into transparent exopolymer particles: Chemical and spectroscopic evidences

Mashura Shammi^{1,2,6}, Xiangliang Pan^{1,5}, Khan M. G. Mostofa³, Daoyong Zhang¹ & Cong-Qiang Liu⁴

Upon exposure to sunlight extracellular polymeric substances (EPS) were partially transformed into transparent exopolymer particles (TEP) and unstable flocs of different sizes without the addition of any precursors. Parallel factor (PARAFAC) modelling of the sample fluorescence spectra identified humic-like and protein-like or tyrosine-like components in both untreated and irradiated EPS samples. After 58 hours of solar irradiation, humic-like substances were entirely decomposed, while the regenerated protein-like substance from EPS was the key component in the irradiated samples. Degradation and reformation of EPS occurred which was confirmed by the results of size exclusion chromatography, dissolved organic carbon, total protein and total polysaccharide analyses. Irradiated EPS was composed of $-\text{COOH}$ or $\text{C}=\text{O}$ (amide I band) and $-\text{NH}$ and $-\text{CN}$ (amide II band), while Fourier transform infrared spectroscopy (FTIR) of TEP revealed more acidic $-\text{COOH}$ and $-\text{C}-\text{O}$ groups, indicating typical acidic protein-like TEP. The regenerated protein-like substances could form complexes with free metals originating from degraded EPS in irradiated samples, which could be responsible for the formation of TEP/floc in the aqueous media. These results suggest that TEP/floc formation from EPS could occur by a complexation mechanism between dissolved organic matter and metals, thereby causing ionic charge neutralisation upon sunlight exposure.

Bacterial biofilms are formed by communities that are embedded in a self-produced matrix of extracellular polymeric substances (EPS)¹, which is a term encompassing a large group of very different biopolymers. The biofilm matrix can be considered an external property of the microorganisms, allowing them to form stable synergistic consortia, supporting interaction with signalling molecules and horizontal gene transfer and, eventually, activation by extracellular enzymes, which turn the matrix into an external digestive system². EPS are a high-molecular-weight ($\text{MW} > 410,000$) mixture of polymers that are composed mainly of polysaccharides, proteins, nucleic acids, lipids, surfactants and humic-like substances^{3,4}. Humic substances are the integral part of the EPS³⁻⁵, which can participate in complexation of trace elements and random flocculation in natural water environments⁶⁻⁹. Therefore, EPS composition can be variable which determines its reactivity and structural

¹Laboratory of Bioremediation, Department of Environmental Pollution and Process Control, Xinjiang Institute of Ecology and Geography, Chinese Academy of Sciences, Urumqi-830011, Xinjiang, P.R. China. ²Department of Environmental Sciences, Jahangirnagar University, Dhaka, 1342, Bangladesh. ³Institute of Surface-Earth System Science, Tianjin University, 92 Weijin Road, Nankai District, Tianjin, 300072, P.R. China. ⁴State Key Laboratory of Environmental Geochemistry, Institute of Geochemistry, Chinese Academy of Sciences, Guiyang, 550002, Guizhou, P.R. China. ⁵College of Environment, Zhejiang University of Technology, Hangzhou, 310014, Zhejiang, P.R. China. ⁶University of Chinese Academy of Sciences, Beijing, 100049, P.R. China. Correspondence and requests for materials should be addressed to X.P. (email: xiangliangpan@163.com) or K.M.G.M. (email: mostofa@tju.edu.cn)

function¹⁰. They provide the mechanical stability of biofilms, mediate their adhesion to surfaces and form a cohesive, three-dimensional polymer network that interconnects and transiently immobilises biofilm cells³. EPS enhances resistance to stress caused by toxicity or environmental variables¹⁰. Biogeochemical cycling of elements—particularly, heavy metals in different chemical forms, mobility, bioavailability and ecotoxicity are significantly influenced by EPS in the aquatic environment⁶. Furthermore, in EPS-dominated biofilm systems, interactions involve both surface complexation to EPS/cells and mineral products of metabolic/abiotic processes¹⁰.

Transparent exopolymeric particles (TEP) are operationally defined as larger than 0.4 µm, whereas the other substances chemically identical to TEP, but smaller than 0.4 µm, can be considered as TEP precursors¹¹. TEP and their precursors are considered as a “planktonic” subgroup of EPS or hydrogel subgroups because they originate via the release of extracellular, acidic polysaccharides produced by phyto-/bacterioplankton^{11,12}. TEP are polysaccharide particles, formed by the aggregation of polymers exuded by phytoplankton and are strongly involved in organic matter sedimentation¹³. Frequently, TEP are intensely colonised by bacteria and other microorganisms, thus serving as hot spots of intense microbial activity and biofilm formation¹⁴. TEP and other microgel particles in marine and freshwaters are part of a size continuum of organic matter that includes polymers, nanogels, microgels, and very large marine (or lake) snow particles (macrogels)¹⁴ that are significant and critical in sedimentation processes¹⁵.

Flocculation is extensively employed for clarification through sedimentation in water treatment works¹⁶. Flocculation has major implications in organic matter (OM) transformation and removal pathways⁷ in aquatic environments. Without chemical reactions dissolved organic matter (DOM) could spontaneously entangle to form particulate organic matter (POM) microgels¹⁷ and correspondingly, photochemical flocculation of terrestrial DOM and Fe⁸. Oftentimes, microbial ferrous iron [Fe(II)] oxidation leads to the formation of iron-rich macroscopic aggregates (“iron snow”) of ferric iron [Fe(III)] in the surface waters depending on surrounding geochemistry¹⁸. Conversely, to understand the kinetics of OM cycling in aquatic environments, it is crucial to achieve a mechanistic and molecular understanding of its transformation processes¹⁹. EPS was transformed into unstable flocs by UV (ultraviolet) radiation and stable flocs by simulated solar radiation of 70 µWcm⁻² (irradiation time 120 min)²⁰. However, the study solely identified turbidity as a precursor to floc formation and many important characteristics behind the flocculation process, i.e., particle size, surface charges, DOC changes and fluorescent component changes were overlooked. Therefore, it is vital to identify physical, chemical and fluorescent characteristics during the transformation processes of EPS to TEP/floc during natural sunlight exposure.

However, the link between photoinduced alteration of EPS and its TEP/floc formation behaviour has received relatively little attention. Therefore, to elucidate the effect of sunlight on EPS photo-flocculation and TEP formation, an experiment was designed to study the formation of TEP from 0.22-µm filtered fraction of EPS. TEP/floc formation was carried out on treated EPS before and after exposure to sunlight at different intervals across the five consecutive days of irradiation. Conventional chemical and spectroscopic methods were used to characterise the TEP/floc formation along with physicochemical changes in the irradiated EPS samples. New insights into the mechanism of photo-flocculation are comprehensively discussed based on the evidences provided from different physical, chemical and spectroscopic analyses of EPS and TEP under natural sunlight conditions.

Results

Photoinduced transformation of EPS to TEP by Alcian blue dye assay. After the extraction of EPS using a 0.22-µm filter, the concentration of TEP obtained was approximately 1.32 ± 0.08 µg/mL xanthan gum (GX) equivalent (Fig. 1A,B). After six hours of sunlight irradiation, the TEP concentration had reached 1.87 ± 0.08 µg/mL GX, which was a 41.7% increase compared to the original sample. However, no significant size change was observed from image analysis during this time (Fig. 2). Within 19 hours and 32 hours TEP concentration varied from 1.96 to 2.16 µg/mL GX equivalents, respectively. Consequently, particle size was more visible (Fig. 2). After 58 hours of sunlight exposure TEP concentration had decreased slightly to 1.35 ± 0.07 µg/mL GX equivalents with more visible particles (Fig. 2D). These results imply that EPS transformed into TEP simultaneously during different timescales upon light exposure and that TEP size increased significantly with increasing time (Fig. 2A,D).

Photo-flocculation of EPS by turbidity, ζ-potential and PSD assay. Turbidity results showed that a significant increase in turbidity of approximately 56.5% with respect to the initial turbidity of the sample was observed after 32 hours of sunlight exposure (Fig. 1A). However, a 47.3% decrease in turbidity was observed after 58 hours. This result is in accordance with that of a previous study, which reported an increase in turbidity from 11.2 to 22.3 NTU within two hours under simulated solar radiation²⁰. It apparently reveals that EPS are decomposed, thereby forming gel-like TEP and floc in aqueous media. Larger floc particles settled on the bottom of the flask, as the turbidity was found to decrease upon light exposure after the 19 hours of exposure. ζ-potential (–mV), the net ionic surface charge of the EPS, varied considerably which indicated the formation of unstable flocs of EPS. However, after the 19 hours of sunlight exposure, ζ-potential decreased to –1.08 (mV), which is approximately a 92% reduction in surface charge compared to the original sample (Fig. 3B). Reducing the magnitude of negative ζ-potential indicates charge neutralisation and destabilisation, which is the well-known conceptual model for the polymer flocculation mechanism^{16,21}.

The role of EPS in the dynamic self-flocculation upon light exposure was observed using particle size distribution (PSD) assay (Fig. 3C). The average PSD of the particles in the extracted EPS was approximately 1000 nm. The polymers in the EPS self-assembled and flocculated to become particles in natural water. This was further justified by a significant decrease of the surface charge (Fig. 3C), which subsequently caused EPS aggregation in the first 6 hours. Such an effect was finally determined to increase particle size by as much as 33% in the treated samples. This implies that each collision between EPS and/or TEP/floc particle resulted in aggregation that leads to particles sticking together as well as breakage. After 58 hours of sunlight exposure particle size was found to

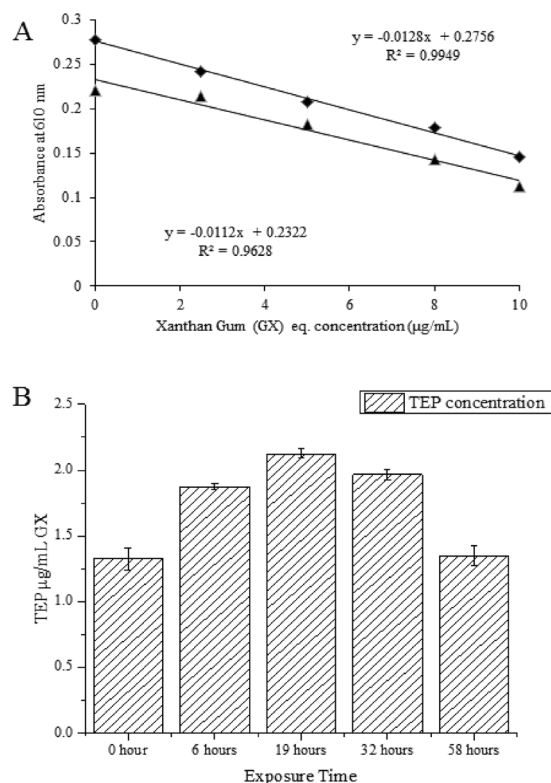


Figure 1. EPS transformation to TEP and flocculation measured as TEP. **A.** TEP calibration curve with Xanthan Gum; **B.** concentration of TEP µg/mL GX (equivalent) during photo exposure under light treatment. Only daylight exposure hours (12 hours per day) were counted, to the exclusion of night hours.

be significantly lower than the original sample by as much as 55.4% (Fig. 3C). This indicates that the polymers of EPS formed flocs by aggregation and disaggregated into smaller particle size of approximately 700 nm by sunlight irradiation. Previously, it was reported that EPS themselves can aggregate to form particles of about 300 nm, regardless of photic conditions²². Furthermore, the UV light intensity which varied from 5–10 Wm⁻² during the experimental day times might be involved in the formation of unstable polymer flocs, followed by subsequent photolysis of the flocs¹⁷. The most important factor affecting the flocculation process is pH^{23,24}. During the irradiation time, the pH changed over the course of the five-day experiment. The original pH (8.78) was decreased gradually reaching 7.91 in the irradiated samples (Fig. 3D). Lowering of the pH may be related to the formation of acidic photoproducts²⁵. However, the finding is in contrast with that of a previous study⁸ where during the irradiation, pH increased; POM and particulate Fe also formed. Such deviations in results could be caused due to variations in the DOM samples.

Changes in the fluorescent substances during photo- and microbial flocculation as identified by EEM-PARAFAC modeling. The results from the PARAFAC modelling on the raw EPS samples demonstrated that the EPS had three fluorescent components. The first fluorescent component represented a combined humic-like (peak M at Ex/Em = 275/399 nm and peak A at Ex/Em = 245/399 nm) and protein-like (peak T at Ex/Em = 275/328 nm and peak T_{UV} at Ex/Em = 255/328 nm) substances (Fig. 4A: Component 1). The second fluorescent component was identified as consisting of humic-like substances with two fluorescence peaks, including peak M at Ex/Em = 320/407 nm and peak A at Ex/Em = 245/407 nm (Fig. 4A: Component 2). The third fluorescent component consisted of unknown substances with two fluorescent peaks, both showing shorter excitation wavelengths (Ex/Em = 225/310 nm and Ex/Em = 225/399 nm, respectively) (Component 3: Fig. 4A; Table 1). Detection of the combined humic-like and protein-like fluorescent components by EEM-PARAFAC modelling was reported in an earlier study²⁶. This could be indicative of the EPS molecular composition, since chemical and spectroscopic studies also generally found EPS to be composed of protein- and humic-like substances^{3,5} along with polysaccharides. It is apparent that humic-like and protein-like substances, two major backbone of EPS molecular structure, could have similar functional groups (–COOH and –NH₂)⁹, which might be responsible to interact with each other and produced combined fluorescent peaks.

The humic-like component in the combined component 1 predominantly showed excitation wavelength maxima (Ex = 275 nm) in the shorter wavelength region compared to the component 2 humic-like substances (Ex = 320 nm). This is assumed to be caused by consequential effects of the interaction of two substances (protein-like and humic-like). To distinguish the protein from the aromatic amino acids (e.g., tryptophan or tyrosine), it was previously shown that the protein-like component is detected at higher fluorescence intensity in the longer wavelength (peak T) region compared to that in the shorter wavelength (peak T_{UV}) region, while for

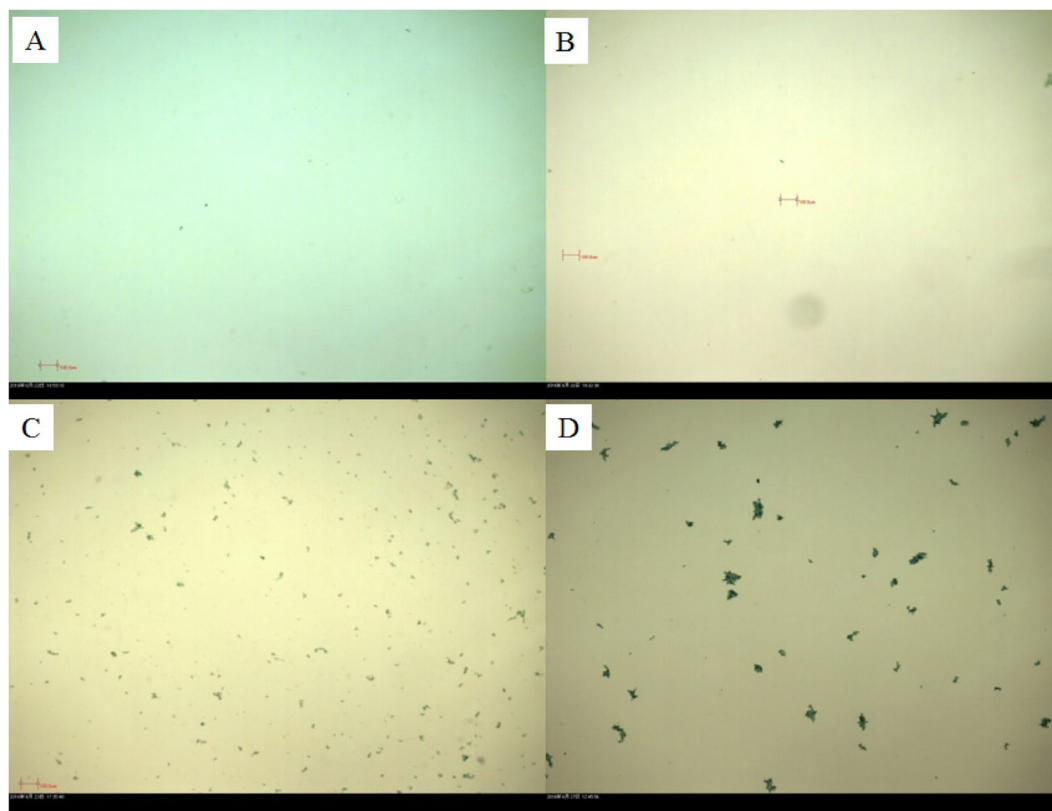


Figure 2. Time-lapse images of EPS to TEP transformation by Alcian Blue dye under sunlight exposures at (A) 0 hour, (B) 6 hours, (C) 19 hours, (D) 58 hours. Only daylight exposure hours (12 hours per day) were counted, to the exclusion of night hours. TEP size varied greatly from less than $2\ \mu\text{m}$ to more than $200\ \mu\text{m}$. All the images were taken at $5\times$ magnification.

tyrosine or tryptophan, fluorescence intensity of peak T is higher than peak T_{UV} ⁹. Component 2 (humic-like) is also termed as “marine humic-like”, because it is often detected in surface waters, particularly in lakes and oceans^{9, 27–30}. Component 3 with unknown fluorescent peaks reported in an earlier study²⁵, could also be a backbone component originated from diverse EPS molecular compositions.

Pursuant to the short-term irradiation of sunlight (1 to 6 hours), EEM-PARAFAC modelling identified three components: protein-like (component 1: peak T at Ex/Em = 275/328 nm and peak T_{UV} at Ex/Em = 245/328 nm), humic-like (component 2: peak M at Ex/Em = 295/405 nm and peak A at 225/405 nm) and tyrosine-like (component 3: peak T at Ex/Em = 265/310 nm and T_{UV} at Ex/Em = 225/310 nm) substances (Fig. 4B; Table 1). These components are similar to components produced from raw EPS except for component 3, which is confirmed as a tyrosine-like component^{9, 27–30} (Fig. 4B). Over six hours of sunlight exposure, the fluorescence intensities of component 1 and component 2 decreased up to 68% and 26%, respectively (Table 1). Upon continuous long-term irradiation of EPS samples between 19 hours and 58 hours, three-component PARAFAC modelling identified mostly a protein-like component 1 with two peaks (peak T at Ex/Em = 275/328 nm and peak T_{UV} at 235/328 nm) and two unknown components (component 2: Ex/Em = 295/474 nm and component 3: Ex/Em = 390/492 nm), which were thought to be photo-products from decomposed humic-like fractions (Fig. 4C; Table 1). The fluorescence intensity of protein-like substances (component 1) was reduced by approximately 62% after 58-hours of irradiation. Fluorescence intensity decreased either by TEP/floc formation through complexation between protein-like substances and trace metals, or through its direct mineralisation into other components. This decrease in fluorescence intensity utterly differs from previous report of stable fluorescence²⁰; presumably due to the application of low-intensity UV. These results further suggest that protein-like substances predominantly remain until the 58 hours of irradiation, which could play an important role in the photo-flocculation processes.

Chemical and molecular-level changes of EPS during photo-flocculation. FTIR analyses of original EPS samples and samples subjected to 58 hours of sunlight irradiation demonstrated that extracted EPS contained several major infrared absorption peaks (Fig. 5A,B). The broad and strong band at approximately 3000 to $3735\ \text{cm}^{-1}$ was observed due to the stretching of the OH existing in all polymers. A weak C–H band at approximately 2938 to $2949\ \text{cm}^{-1}$ indicates the C–H stretching vibration of methyl and methylene groups. Other major peak regions include 400 to $921\ \text{cm}^{-1}$, similar to carbohydrates and polysaccharides consequent to glycosidic linkage. A distinct difference was observed in the peak position at $672\ \text{cm}^{-1}$ which was found to disappear for the 32 to 58-hour irradiated sample, indicating breakage of the glycosidic linkage of the polysaccharide³⁰. Another major peak at $1124\ \text{cm}^{-1}$ observed in irradiated and raw EPS samples may indicate the S = O and C–O–S³¹.

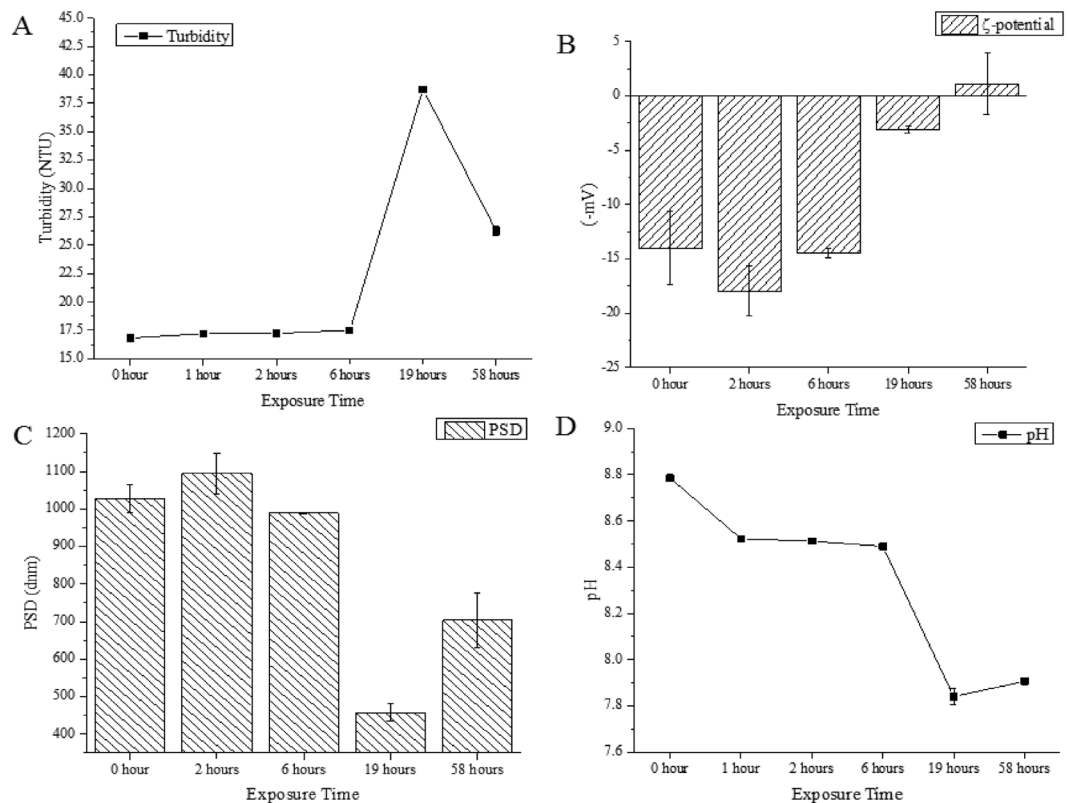


Figure 3. EPS transformation to TEP and flocculation measured as: (A) photo-flocculation of EPS upon light exposure, measured as turbidity (NTU); (B) ζ -potential ($-mV$) of light exposure; (C) particle size distribution (dnm) of EPS treated in sunlight; (D) changes in pH of EPS in light conditions after exposure in sunlight. Only daylight exposure hours (12 hours per day) were counted, to the exclusion of night hours.

Proteins are shown by the distinct peak positions at $1576-1585\text{ cm}^{-1}$ in raw EPS samples and $1617-1640\text{ cm}^{-1}$ in irradiated EPS samples, which may belong to the amide I band and are assignable to $C=O$ of the $-COOH$ stretching vibration. Amide II is shown by the two bands at 1435 cm^{-1} to 1446 cm^{-1} , which are assigned to the $N-H$ deformation and $C-N$ stretching in $-CO-NH-$. A distinct peak position was observed at 1382 cm^{-1} , which appeared after 19 hours of irradiation and remained sharper after 58 hours. This indicates the presence of symmetrical stretching of $C=O$ in a $-COO^-$ group³². Moreover, the FTIR spectrum of 58-hour irradiated TEP/floc which was collected on the $0.22\text{-}\mu\text{m}$ membrane, revealed that, unlike the original EPS, the TEP/floc was characterised by more acidic protein-like components containing $-COOH$ or $C=O$ groups assigned to 1638 cm^{-1} and 1384 cm^{-1} (Fig. 5B). It is well known that amide linkages generally constitute a defining molecular structural feature of proteins. Alcian blue dyes stain the carboxyl and sulphate half-ester groups of the acidic polymers³³. Moreover, photochemically flocculated POM was enriched in amide functionality⁸. These results therefore imply that TEP/floc could have been formed from protein-like components originating from the EPS upon light exposure.

During the sunlight irradiation and flocculation, dissolved organic carbon (DOC), total protein and total polysaccharide reduction further confirmed mineralisation of the EPS (Fig. 6A,B). A small decrease in the DOC concentration was detected during the first six hours ($\sim 9.5\%$) of irradiation compared to the original DOC ($308.97 \pm 1.2\text{ mgL}^{-1}$). This decreasing trend was substantially higher as irradiation time increased and ultimately, a 38.4% decrease was detected after 58 hours of irradiation (Fig. 6A). The degradation of DOC was reported in previous studies^{9,34} and that 7% of the terrestrial DOM of DOC was converted to POC, while 75% was remineralised⁸. A 59% reduction in total protein and a 73% reduction in total polysaccharides were observed after 58 hours of irradiation (Fig. 6B).

To observe changes in protein molecular weight, standard protein and its molecular weight peak were used for the light-treated EPS with respect to the original EPS. According to the retention times and appearances of peaks, four peak positions were considered with the probable molecular weight of $>94.7\text{ kDa}$, $94.7-66.2\text{ kDa}$, $45-33\text{ kDa}$ and $20-14.4\text{ kDa}$. The original EPS without sunlight exposure included three distinct peak positions $>94.7\text{ kDa}$, $94.7-66.2\text{ kDa}$ and $45-33\text{ kDa}$ with an area of approximately 2%, 5% and 82%, respectively. After 19-hours of irradiation, the $45-33\text{ kDa}$ peak was found to increase with regard to its percentage area of 84.2%. However, 58-hours of irradiation caused the $94.7-66.2\text{ kDa}$ peak to break into two peaks with approximate areas of 11% and 12%, while the peak of $45-33\text{ kDa}$ had decreased to 14.3% (Fig. 6C). The peaks representative of the high-molecular-weight fractions for the original EPS was decreased in intensities. This result implies a net decrease in molecular weight, which could belong to the low-molecular-weight organic acids²⁵. Such changes

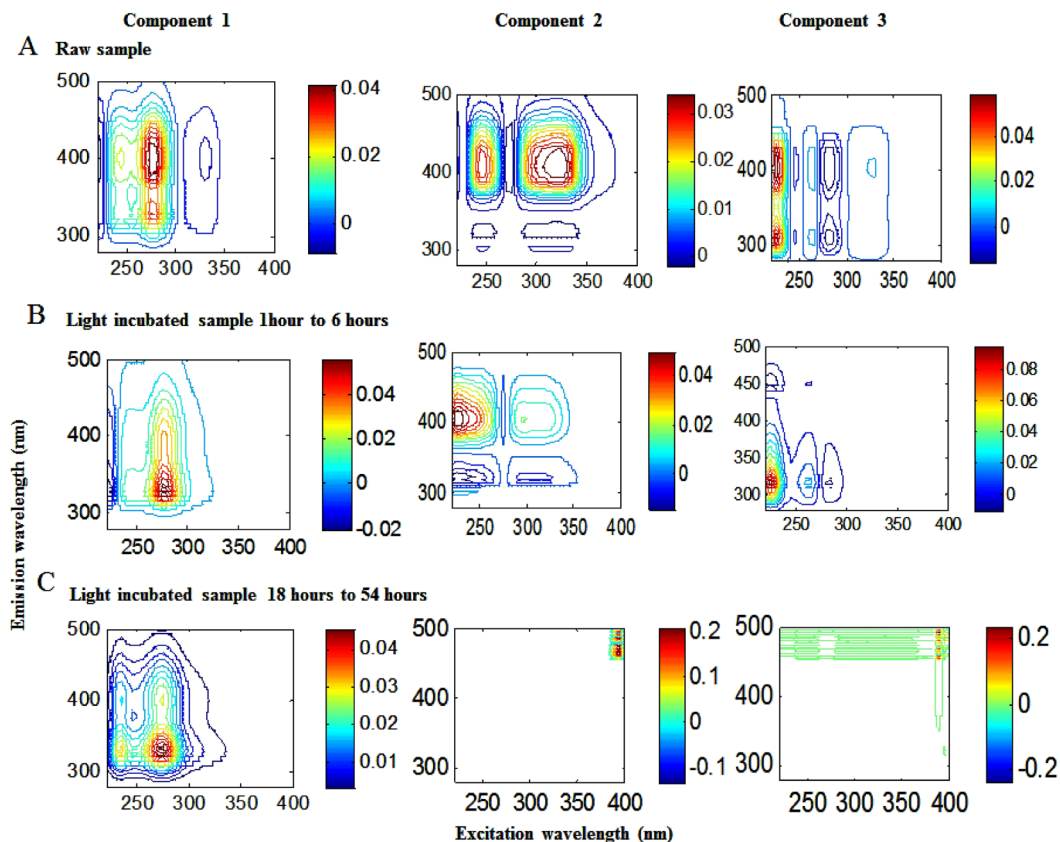


Figure 4. Fluorescent components of EEM-PARAFAC identified by three-component analysis for: (A) Raw EPS samples, (B) sunlight irradiated EPS sample from 1 hour to 6 hours and (C) sunlight irradiated EPS sample from 19 hours to 58 hours of exposure. Only daylight exposure hours (12 hours per day) were counted, to the exclusion of night hours.

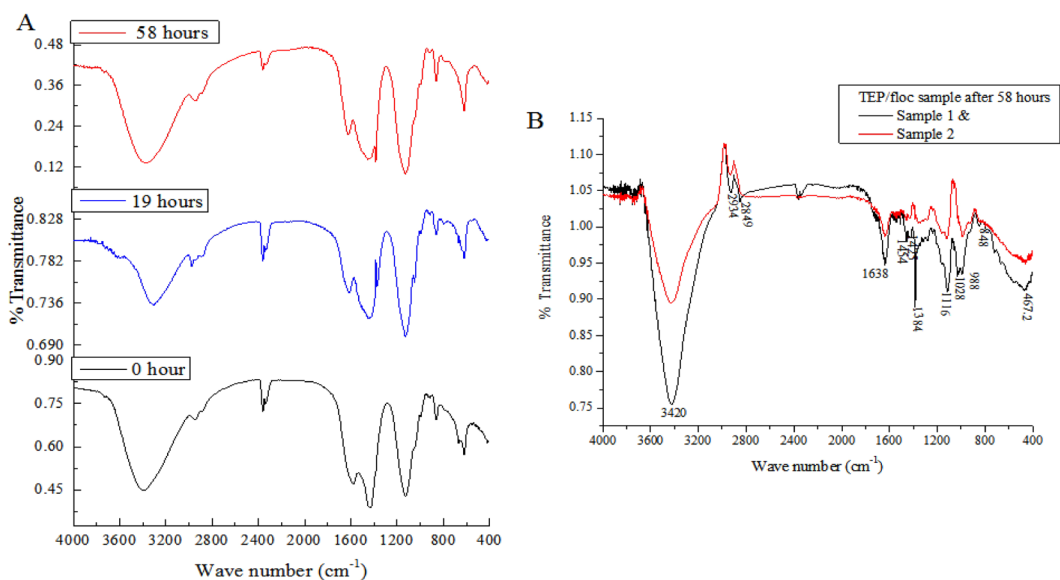


Figure 5. (A) FTIR spectrum of EPS with photo exposure at 0 hour, 19 hours and 58 hours; (B) FTIR spectrum of TEP/floc filtered on 0.22 μm filter after 58 hours of photo exposure. Only daylight exposure hours (12 hours per day) were counted, to the exclusion of night hours. It is evident from the two figures that compared to the original and light exposed EPS; TEP/flocs collected on 0.22 μm membrane filter contained more acidic protein-like functional groups.

Components	Excitation and emission maxima (% decrease in fluorescence intensity)	Description	Peak region	Corresponding description in the earlier study
Raw EPS sample fluorescence properties in this study				
Component 1 ⁵²	275/328 and	Protein-like	Peak T	280–300/328–356 nm ⁹
	245/328		Peak T _{UV}	235–250/338–356- nm ⁹
	275/399 and	Humic-like	Peak M	260/423–428 nm ²⁹ ; 290–330/358–434 nm ⁹
	245/399		Peak A	250–260/380–480 ²⁹ ; 225–260/358–416 ⁹
Component 2	320/407 and	Humic like	Peak M	260/423–428 nm ²⁹ ; 322/407 nm ²⁷ ; 290–330/358–416 nm ⁹
	245/407		Peak A	250–260/380–480 nm ²⁹ ; 225–260/358–416 nm ⁹
Component 3 ⁵²	225/399 and	Unknown components	Peak A	This study
	225/260		Peak T _{UV}	This study
Photochemical degradation (1 hour to 6 hours) in this study				
Component 1	275/328 and (–68%)	Protein-like	Peak T	280–300/328–356 nm ²⁷
	245/328–68%		Peak T _{UV}	235–250/338–356- nm ²⁷
Component 2	295/405 and –26%	Humic-like	Peak M	262/380–420 nm ²⁹ ; 322/407 nm ²⁷ ; 290–330/358–434 nm ⁹
	225/405 –26%		Peak A	260/380–460 nm ²⁹ ; 225–260/358–416 nm ⁹
Component 3	265/260 and (–68%)	Tyrosine-like	Peak T	265–280/293–213 nm including standard tyrosine ³⁰ ; 270–280/293–264 nm ²⁷
	225/260 (–44%)		Peak T _{UV}	230/304–307 nm including standard Tyrosine ²⁷
Photochemical degradation (19 hours to 58 hours) in this study				
Component 1	275/328 (–62%)	Protein-like	Peak T	280–300/328–356 nm ⁹
	235/328 (–62%)		Peak T _{UV}	235–250/338–356- nm ⁹
Component 2	295/474	Unknown photo-products	Peak C	No reference
Component 3	390/272	Unknown photo-products	Peak C	No reference

Table 1. Fluorescence excitation/emission (Ex/Em) wavelengths of the raw and treated EPS and the subsequent characteristic peaks of the reference components. (+) and (–): an increase and a decrease in fluorescence intensities (%) of various peaks, respectively due to solar and microbial effects. The percentage changes in the fluorescence intensities of various components are estimated by comparing the treated samples with raw EPS samples (before irradiation). Only daylight exposure hours (12 hours per day) were counted, to the exclusion of night hours.

in the protein-molecular-weights are in agreement with changes in pH, fluorescence, FTIR spectrum and total protein analysis, as discussed earlier, thereby forming TEP/floc.

Discussion

A conceptual model of the photoinduced flocculation of EPS. Based on the results, we obtained in this study, we propose a conceptual model for the formation of TEP/floc from the photoinduced EPS (Fig. 7). According to this model, the molecular compositions of EPS, when decomposed, can form new protein-like components. Such newly formed protein-like components can form complexes with free metals produced from the photodegradation of EPS and its molecular components. Metal-protein complexation is a well-known phenomenon in both water-based and biological systems^{6,9,35–40}. Correspondingly, our proposed model is supported by earlier studies wherein proteins have been shown to form aggregates at low metal ion concentrations^{37,38,41}. However, our model is partly inconsistent with the previous mechanism of photo-flocculation of bulk DOM first provided by Helms and his colleagues⁸, which is possibly attributed to not identifying the molecular composition of the DOM and its photic end-products. Helms and his colleagues suggested that photo-flocculation occurred via two or more pathways. They reported that initial flocculation of organic and inorganic material might not occur simultaneously. In asserting a mechanism, they also proposed that during “Phase I” organic matter flocculates but that Fe does not. During “Phase II” both organic matter and Fe flocculate. There is some lack of understanding of this mechanism that does not fit well with the current knowledge of photochemistry. For example, it is generally known that DOM, including EPS is photochemically decomposed, particularly in the case of humic substances (e.g., fulvic and humic acids) upon sunlight exposure in natural waters^{34,42–46}. This ultimately produces low-molecular-weight DOM²⁵ and mineralisation of other products, such as CO₂, DIC (dissolved CO₂, H₂CO₃, HCO₃[–] and CO₃^{2–}), NH₄⁺ and PO₄^{3–}^{9,47,48}. Such decomposition of DOM was not supported by the aforementioned mechanism. The second issue is that over 99% of dissolved Fe is strongly complexed with the functional groups of DOM in marine waters^{49–51}. In essence, high-molecular-weight DOM including EPS, often exists as complexation with trace metals (M), such as, DOM-M or EPS-M in natural waters, which also did not appear in the aforementioned mechanism. FTIR and SEC analysis of TEP/flocs in our study demonstrated that TEP/flocs

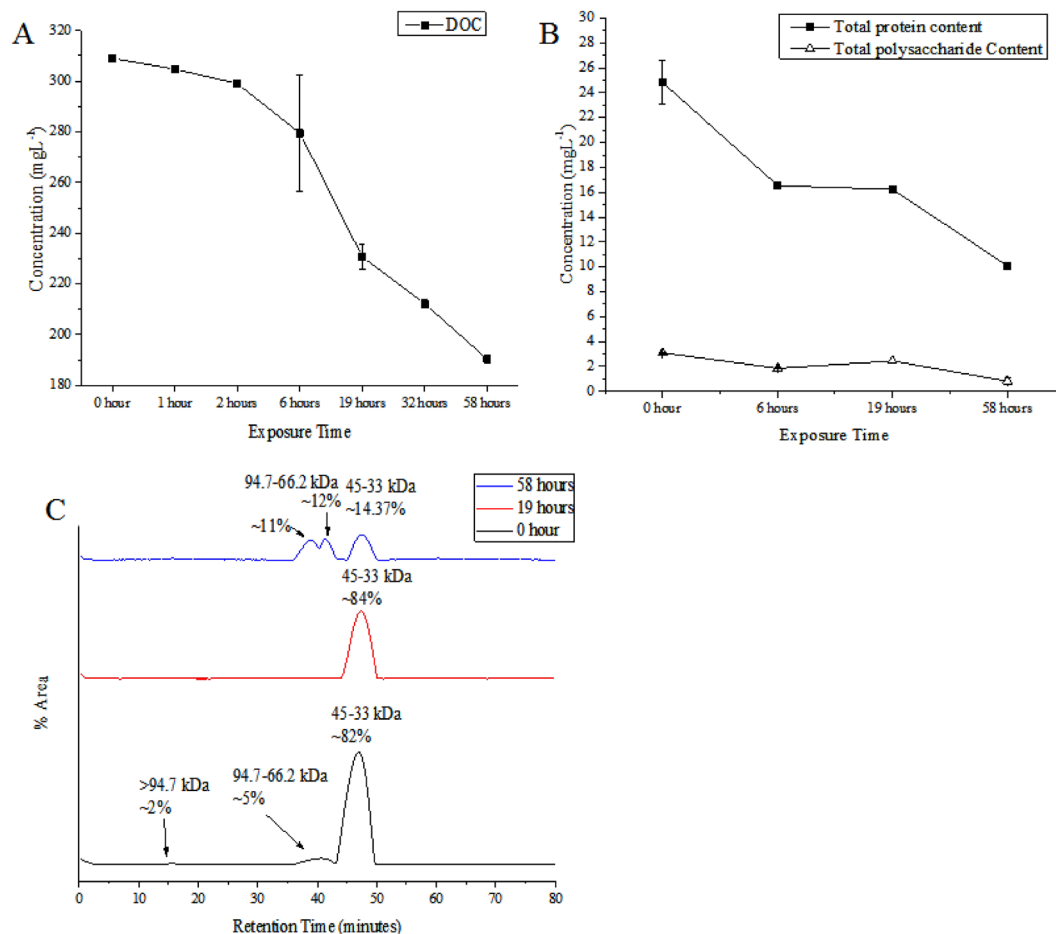


Figure 6. Influences of sunlight on photo-degradation of (A) DOC mgL⁻¹ content of EPS under light condition; (B) changes in total protein and total polysaccharide concentration during the exposure time and (C) Fingerprints of EPS protein molecular weight regions at 0 hour, 19 hours and 58 hours. Only daylight exposure hours (12 hours per day) were counted, to the exclusion of night hours.

were composed of organic acid-linked structural phenomena which were protein dominant. Correspondingly, formation of protein-like or tyrosine-like substances (as identified from EEM-PARAFAC modelling) in irradiated samples is crucial for better understanding of this mechanism. As discussed earlier the protein-like substances can form complexes with metals. The third issue is that our time-lapse images of the EPS-to-TEP-size transformation showed that TEP/floc formation in aqueous solution is gradually increased from the 0 hour to the 58-hour time points.

Proposed mechanisms of photo-flocculation. Considering the above mentioned issues, we suggest that a simultaneous process could link TEP/floc formation to the degradation of EPS (or DOM) in aqueous media, thereby forming complexes between free metals and newly formed DOM that ultimately generate TEP/flocs. In these mechanism, the initial complex between EPS and metal abbreviated as EPS-M upon light exposure can produce protein-like and humic-like substances and unknown components, any of which are considered to be complexed with metals in the solution (Eqs 1–2). Interestingly, EPS raw solution contained high contents of different trace metals, such as Fe (905.9 ppb), Zn (20.2 ppb), Al (5.6 ppb), Ni (25.3 ppb), Cr (7.1 ppb), As (70.1 ppb), Ba (30.4 ppb), Pb (0.8 ppb) and Cd (0.02 ppb) in this study and depending on the complexation capacity of the metals, they formed complexes with EPS. Such EPS-M complexation has been reported in earlier studies^{6,21–41}. However, after 58 hours of irradiation, all humic-like substances were entirely decomposed (Fig. 4), while the remaining protein-like substances could complex with free metals, which could correspondingly form the TEP/floc. Because TEP/floc is composed of organic substances exhibiting various functional groups (–COOH, –C=O, –OH etc.) identified by FTIR spectra (Fig. 5A,B), they could be produced either via the complexation of PLS-M, HLS-M and UC-M produced during rearrangement of PLS, HLS and/or their photodegradation (Eq. 3). Where, PLS, HLS and UC are the protein-like substances, humic-like substances, unknown components and their complexes with metals are PLS-M, HLS-M and UC-M, respectively. Note that the humic-like substance was completely decomposed and it played a minor role in flocculation processes other than as an electron acceptor and donor^{3,5}. The protein like substance^{3,5}, unknown components and the unknown photo-products could be responsible for TEP/floc formation. Therefore, given EPS as autochthonous DOM and its complexations with

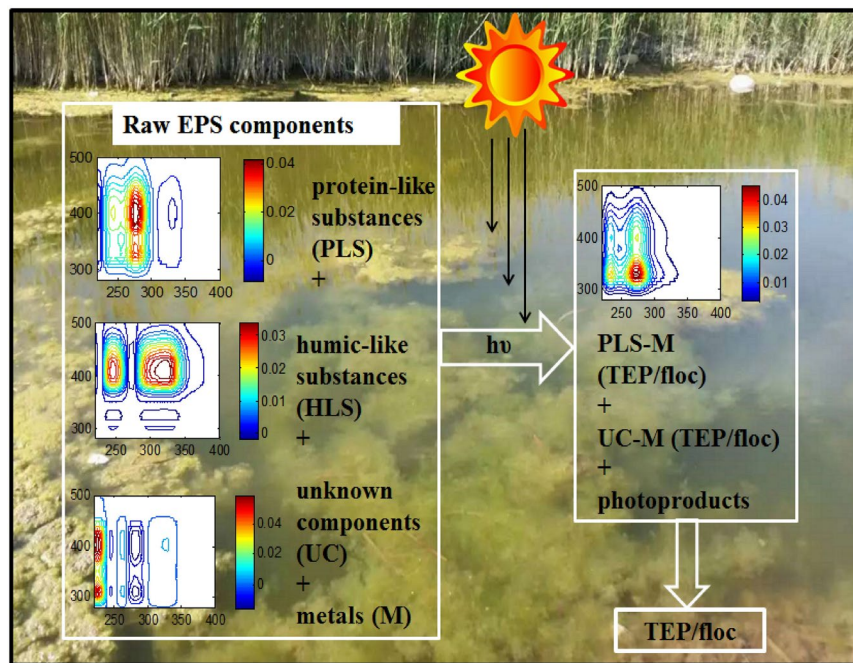
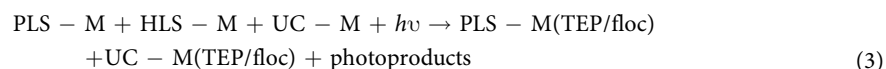
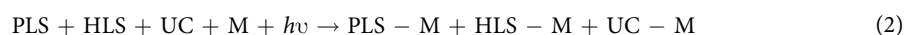


Figure 7. A conceptual model of TEP/floc formation from raw EPS components. Where PLS, HLS and UC are the protein-like substances, humic-like substances, unknown components and their complexes with metals are PLS-M, HLS-M and UC-M, respectively. Photo-flocculation could occur simultaneously along with photoinduced EPS (or DOM) in aqueous media, thereby forming complexes between free metals and newly formed DOM (photoproducts) that ultimately generate TEPs/flocs. During the end of the processes, humic-like substances are completely decomposed, and their ability to form floc/TEP is decreased. Protein-like substances of EPS predominantly participate in TEP/flocculation processes.

trace metals (M) abbreviated as EPS-M, the possible detailed mechanistic sequence of TEP/floc formation by sunlight is as follows (Eqs 1–3):



Similar reaction mechanisms are reported for DOM-M degradation, where Fe^{3+} -DOM complexes are decomposed because of the rapid excitation of π -electron bonding upon light exposure^{34,44–46}. During photochemical flocculation of the DOM and iron to POM, approximately 87% of the iron was removed from the dissolved phase after 30 days. However, iron did not flocculate until a major fraction of the DOM was removed by photochemical degradation and flocculation (>10 days); thus, during the initial 10 days, there were sufficient organic ligands present or the pH was low enough to keep iron in solution⁸. Note that the Fe^{3+} -DOM complex would be formed by the donation of electrons from O- or S-containing functional groups of DOM, mostly humic substances (fulvic and humic acids)⁹ to an outer unpaired *d*-orbital of Fe^{3+} ($^{25}\text{Fe}^{2+}$: $1s^2 2s^2 2p^6 3s^2 3p^6 3d^2_{xy} 3d^2_{xz} 3d^1_{yz} 3d^1_{x^2-y^2} 3d^1_{z^2} 4s^0$) and Al^{3+} ($1s^2 2s^2 2p^6 3d^3 3s^0 3p_x^0 3p_y^0 3p_z^0$). Due to the presence of protein-like components in the sample irradiated for 58-hours, free trace metals preferentially form complexes with only newly formed protein-like substances (Fig. 4C), thereby forming metal ion complexation between protein-like or unknown DOM components and dissolved Fe or Al or colloids of EPS. Such metal-protein (or DOM molecules) complexation is reported in earlier studies^{6,9,38,40,52}, thereby forming aggregation^{8,15,37,38,53}. Metal-protein binding is often observed through C=O or C–N with the precipitation of tyrosine residues³⁸. Although photo-flocculation of the EPS occurred throughout 58 hours of sunlight exposure, all the Fe and Al essentially remained in the solution because of the complete decomposition of the humic-like substances and either partial degradation or TEP/floc formation of protein-like substances. Because EPS is considered to be complexed with metals (e.g. Fe), it is either quickly recycled back into the dissolved phase by complexation with protein-like substances, or it photo-reduced to Fe (II), which was soluble in the experimental pH condition⁸. Rapid decomposition of EPS-M complexes is considered to take place due to a rapid excitation from its π -electron bonding system upon light exposure⁹. It can be noted that lectin-like proteins of EPS might be responsible for aggregation and floc formation^{5,51}.

This study confirms that EPS can form TEP and flocculates in the presence of sunlight. Increasing TEP concentrations can result in further significant accumulation of carbon-rich components that subsequently enhance sedimentation of POM⁵³. TEP/floc thus plays an important role in recirculation as an additional source of nutrients, trace elements and DOM to the water column from deep sediment in the winter season, which is a result of vertical mixing in surface waters, particularly in lakes and oceanic environments^{9,54}. Finally, when considering the peak formation of TEP after 19-hours (2nd day) of photo exposure (Fig. 1B), with its successive decrease in concentration from the 32 hours to 58 hours (3rd to 5th day). It is notable that total cumulative sunlight illuminated intensity was ~7216 MJ/m² with frequency >0.43–1.50 × 10⁶ GHz on the second day and a total illuminated intensity of 7701 MJ/m² (counting solar intensity at every minute) thereafter. These findings suggest that flocs/TEP can be formed and be stable at first 19-hours and then decompose successively. Such an assessment could be supported by the turbidity and other observations (Fig. 3A), for which the highest turbidity is observed after 19-hours and then decreases subsequently. *In-situ* experiments are important to further confirm the stability of flocs/TEP in lake or oceanic environments, which could offer foci for further research. In essence, the detection of fluorescent components using a combination of EEM-PARAFAC modelling is an important paradigm for better understanding TEP/floc formation from EPSs under the irradiation processes.

Methods

Collection of the microbial mat. Bosten Lake in Kuerle, Xinjiang Province, China, is an interesting ecosystem in so far as the salinity gradient flows from fresh to sub-saline. Microbial mat samples of alga-bacteria rich in EPS were collected from the pond west of Bosten Lake (N 42° 01.269' and E 86° 47.293') (Supplementary Fig. 1) on the 28th of November 2014. The temperatures on the date of sample collection varied from (−4° to −12 °C). The frozen mat samples were collected in a container and immediately transported to the Xinjinan Institute of Ecology and Geography and preserved at −20 °C.

The remaining details for the experimental design for photo-flocculation, extraction and characterisation of EPS and all analytical methods are reported in the Supplementary Information.

References

- Flemming, H. C. *et al.* Biofilms: an emergent form of bacterial life. *Nat. Rev. Microbiol.* **14**, 563–575 (2016).
- Flemming, H. C. The perfect slime. *Colloids Surf B.* **86**, 251–259 (2011).
- Flemming, H. C. & Wingender, J. The biofilm matrix. *Nat. Rev. Microbiol.* **8**, 623–633 (2010).
- Sheng, G. P., Yu, H. Q. & Li, X. Y. Extracellular polymeric substances (EPS) of microbial aggregates in biological wastewater treatment systems: a review. *Biotechnol. Adv.* **28**, 882–894 (2010).
- More, T. T. *et al.* Extracellular polymeric substances of bacteria and their potential environmental applications. *J. Environ. Manage.* **144**, 1–25 (2014).
- Zhang, D. *et al.* Complexation between Hg(II) and biofilm extracellular polymeric substances: an application of fluorescence spectroscopy. *J. Hazard. Mater.* **175**, 359–365 (2010).
- Asmala, E. *et al.* Qualitative changes of riverine dissolved organic matter at low salinities due to flocculation. *J. Geophys. Res. Biogeosci.* **119**, 1919–1933 (2014).
- Helms, J. R., Mao, J., Schmidt–Rohr, K., Abdulla, H. & Mopper, K. Photochemical flocculation of terrestrial dissolved organic matter and iron. *Geochim. Cosmochim. Acta* **121**, 398–413 (2013).
- Mostofa, K. M. G., Yoshioka, T., Mottaleb, A. & Vione, D. Photobiogeochemistry of organic matter: Principles and practices in water environments. (Springer, 2013).
- Tourney, J. & Ngwenya, B. T. The role of bacterial extracellular polymeric substances in geomicrobiology. *Chem. Geol.* **386**, 115–132 (2014).
- Villacorte *et al.* Improved method for measuring transparent exopolymer particles (TEP) and their precursors in fresh and saline water. *Water Res.* **70**, 300–312 (2015).
- Bar–Zeev, E., Passow, U., Romero–Vargas Castrillon, S. & Elimelech, M. Transparent exopolymer particles: from aquatic environments and engineered systems to membrane biofouling. *Environ. Sci. Technol.* **49**, 691–707 (2015).
- Bourdin *et al.* Dynamics of transparent exopolymeric particles and their precursors during a mesocosm experiment: Impact of ocean acidification. *Estuar. Coast Shelf Sci.* **186**, 112–124 (2017).
- Bar–Zeev, E., Berman–Frank, I., Girshevitz, O. & Berman, T. Revised paradigm of aquatic biofilm formation facilitated by microgel transparent exopolymer particles. *Proc. Natl. Acad. Sci. USA* **109**, 9119–9124 (2012).
- Verdugo, P. *et al.* The oceanic gel phase: a bridge in the DOM-POM continuum. *Mar. Chem.* **92**, 67–85 (2004).
- Lee, C., Chong, M., Robinson, J. & Binner, E. A review on development and application of plant–based biofloculants and grafted biofloculants. *Ind. Eng. Chem. Res.* **53**, 18357–18369 (2014).
- Chin, W.–C., Orellana, M. V. & Verdugo, P. Spontaneous assembly of marine dissolved organic matter into polymeric gels. *Nature* **391**, 568–572 (1998).
- Lu, S. *et al.* Insights into the structure and metabolic function of microbes that shape pelagic iron-rich aggregates (“iron snow”). *App. Environ. Microbiol.* **79**, 4272–4281 (2013).
- Koch, B. P., Kattner, G., Witt, M. & Passow, U. Molecular insights into the microbial formation of marine dissolved organic matter: recalcitrant or labile? *Biogeosciences* **11**, 4173–4190 (2014).
- Song, W. *et al.* Effects of irradiation and pH on fluorescence properties and flocculation of extracellular polymeric substances from the cyanobacterium *Chroococcus minutus*. *Colloids Surf. B* **128**, 115–118 (2015).
- Hjorth, M. & Jørgensen, B. U. Polymer flocculation mechanism in animal slurry established by charge neutralization. *Water Res.* **46**, 1045–1051 (2012).
- Zhang, S. *et al.* Aggregation, dissolution, and stability of quantum dots in marine environments: importance of extracellular polymeric substances. *Environ. Sci. Technol.* **46**, 8764–8772 (2012).
- Schlesinger, A. *et al.* Inexpensive non-toxic flocculation of microalgae contradicts theories; overcoming a major hurdle to bulk algal production. *Biotechnol. Adv.* **30**, 1023–1030 (2012).
- Spilling, K., Seppälä, J. & Tamminen, T. Inducing autoflocculation in the diatom *Phaeodactylum tricorutum* through CO₂ regulation. *J. Appl. Phycol.* **23**, 959–966 (2010).
- Lou, T. & Xie, H. Photochemical alteration of the molecular weight of dissolved organic matter. *Chemosphere* **65**, 2333–42 (2006).
- Shammi, M. *et al.* Seasonal variations and characteristics differences in the fluorescent components of extracellular polymeric substances from mixed biofilms in saline lake. *Sci. Bull.* **62**, 764–766 (2017).

27. Wang, Z.-G. *et al.* Composition analysis of colored dissolved organic matter in Taihu Lake based on three dimension excitation-emission fluorescence matrix and PARAFAC model, and the potential application in water quality monitoring. *J. Environ. Sci.* **19**, 787–791 (2007).
28. Borisover, M., Laor, Y., Parparov, A., Bukhanovsky, N. & Lado, M. Spatial and seasonal patterns of fluorescent organic matter in Lake Kinneret (Sea of Galilee) and its catchment basin. *Water Res.* **43**, 3104–3116 (2009).
29. Coble, P. Characterization of marine and terrestrial DOM in sea water using excitation-emission matrix spectroscopy. *Mar. Chem.* **51**, 325–346 (1996).
30. Yamashita, Y. & Tanoue, E. Distribution and alteration of amino acids in bulk DOM along a transect from bay to oceanic waters. *Mar. Chem.* **82**, 145–160 (2003).
31. Singh, R. P. *et al.* Isolation and characterization of exopolysaccharides from seaweed associated bacteria *Bacillus licheniformis*. *Carbohydr. Polym.* **84**, 1019–1026 (2011).
32. Omoike, A. & Chorover, J. Spectroscopic study of extracellular polymeric substances from *Bacillus subtilis*: aqueous chemistry and adsorption effects. *Biomacromolecules* **5**, 1219–1230 (2004).
33. Passow, U. & Alldredge, A. L. A dye-binding assay for the spectrophotometric measurement of transparent exopolymer particles (TEP). *Limnol. Oceanogr.* **40**, 1326–1335 (1995).
34. Moran, M. A., Sheldon, W. M. Jr. & Zepp, R. G. Carbon loss and optical property changes during long-term photochemical and biological degradation of estuarine dissolved organic matter. *Limnol. Oceanogr.* **45**, 1254–1264 (2000).
35. Barnard, A. *et al.* Selective and potent proteomimetic inhibitors of intracellular protein–protein interactions. *Angew. Chem., Int. Ed.* **54**, 2960–2965 (2015).
36. Li, G. *et al.* G. Binding states of protein–metal complexes in cells. *Anal. Chem.* **88**, 10860–10866 (2016).
37. Tamás, M. J. *et al.* Heavy metals and metalloids as a cause for protein misfolding and aggregation. *Biomolecules* **4**, 252–267 (2014).
38. Nahar, S. & Tajmir-Riahi, H. A. Complexation of heavy metal cations Hg, Cd, and Pb with proteins of PSII: Evidence for metal–Sulfur binding and protein conformational transition by FTIR spectroscopy. *J. Colloid Interface Sci.* **178**, 648–656 (1996).
39. Gerbino, E. *et al.* FTIR spectroscopy structural analysis of the interaction between *Lactobacillus kefir* S-layers and metal ions. *J. Mol. Struct.* **987**, 186–192 (2011).
40. Shoukry, A. A. Complex formation reactions of (2,2'-dipyridylamine)copper(II) with various biologically relevant ligands. The kinetics of hydrolysis of amino acid esters. *Transit. Metal Chem.* **30**, 814–827 (2005).
41. Jacobson, T. *et al.* Arsenite interferes with protein folding and triggers formation of protein aggregates in yeast. *J. Cell Sci.* **125**, 5073–5083 (2012).
42. Kopáček, J., Klemntova, S. & Norton, S. Photochemical production of ionic and particulate aluminum and iron in lakes. *Environ. Sci. Technol.* **39**, 3656–3662 (2005).
43. Mostofa, K. M. G. & Sakugawa, H. Simultaneous photoinduced generation of Fe(2+) and H₂O₂ in rivers: An indicator for photo-Fenton reaction. *J. Environ. Sci. (China)* **47**, 34–38 (2016).
44. Vione, D. *et al.* Sources and sinks of hydroxyl radicals upon irradiation of natural water samples. *Environ. Sci. Technol.* **40**, 3775–3781 (2006).
45. White, E. M., Vaughan, P. P. & Zepp, R. G. Role of the photo-Fenton reaction in the production of hydroxyl radicals and photobleaching of colored dissolved organic matter in a coastal river of the southeastern United States. *Aquat. Sci.* **65**, 402–414 (2003).
46. Granéli, W., Lindell, M. & De Farria, B. M. & De Assis Esteves, F. Photoproduction of dissolved inorganic carbon in temperate and tropical lakes—dependence on wavelength band and dissolved organic carbon concentration. *Biogeochemistry* **43**, 175–195 (1998).
47. Ma, X. & Green, S. A. Photochemical transformation of dissolved organic carbon in Lake Superior—an *in-situ* experiment. *J. Great Lakes Res.* **30**, 97–112 (2004).
48. Hopwood, M. J., Statham, P. J., Skrabal, S. A. & Willey, J. D. Dissolved iron(II) ligands in river and estuarine water. *Mar. Chem.* **173**, 173–182 (2015).
49. Kondo, Y., Takeda, S. & Furuya, K. Distinct trends in dissolved Fe speciation between shallow and deep waters in the Pacific Ocean. *Mar. Chem.* **134–135**, 18–28 (2012).
50. Su, H., Yang, R., Zhang, A. & Li, Y. Dissolved iron distribution and organic complexation in the coastal waters of the East China Sea. *Mar. Chem.* **173**, 208–221 (2015).
51. Park, C. & Novak, J. T. Characterization of lectins and bacterial adhesions in activated sludge flocs. *Water Environ. Res.* **81**, 755–764 (2009).
52. Pereira, S. *et al.* Using extracellular polymeric substances (EPS)-producing cyanobacteria for the bioremediation of heavy metals: do cations compete for the EPS functional groups and also accumulate inside the cell? *Microbiology* **157**, 451–458 (2011).
53. Engel, A. *et al.* Impact of CO₂ enrichment on organic matter dynamics during nutrient induced coastal phytoplankton blooms. *J. Plankton Res.* **36**, 641–657 (2014).
54. Tremblay, J.-É. *et al.* Impact of river discharge, upwelling and vertical mixing on the nutrient loading and productivity of the Canadian Beaufort Shelf. *Biogeosciences* **11**, 4853–4868 (2014).

Acknowledgements

This work was financially supported by National Natural Science Foundation of China (41203088, 31360027, U1120302, and 21177127). This study was also partly supported by the Key Construction Program of the National “985” Project, Tianjin University, China. *Mashura Shammi* was awarded by the “CAS–TWAS President’s Fellowship program 2013”. We acknowledge Xinjiang Uygur Autonomous Region Meteorological Bureau for kindly providing hourly solar radiation intensity data and also Prof. Wenjuan Song, Xinjiang Institute of Ecology and Geography, for all the communication with Xinjiang Uygur Autonomous Region Meteorological Bureau.

Author Contributions

X.L.P. and K.M.G.M. designed and planned the experiment. M.S. conducted the experiments and analysed the results. M.S. and K.M.G.M. wrote the manuscript. All authors discussed the results and reviewed the manuscript at all stages. All authors confirmed on the final version of the manuscript.

Additional Information

Supplementary information accompanies this paper at doi:10.1038/s41598-017-09066-8

Competing Interests: The authors declare that they have no competing interests.

Publisher’s note: Springer Nature remains neutral with regard to jurisdictional claims in published maps and institutional affiliations.



Open Access This article is licensed under a Creative Commons Attribution 4.0 International License, which permits use, sharing, adaptation, distribution and reproduction in any medium or format, as long as you give appropriate credit to the original author(s) and the source, provide a link to the Creative Commons license, and indicate if changes were made. The images or other third party material in this article are included in the article's Creative Commons license, unless indicated otherwise in a credit line to the material. If material is not included in the article's Creative Commons license and your intended use is not permitted by statutory regulation or exceeds the permitted use, you will need to obtain permission directly from the copyright holder. To view a copy of this license, visit <http://creativecommons.org/licenses/by/4.0/>.

© The Author(s) 2017